Heterogeneous Catalysis

DOI: 10.1002/anie.200906675

Evidence for the Surface-Catalyzed Suzuki–Miyaura Reaction over Palladium Nanoparticles: An Operando XAS Study**

Peter J. Ellis, Ian J. S. Fairlamb, Simon F. J. Hackett, Karen Wilson, and Adam F. Lee**

The nature of the active catalytic species in palladium-catalyzed cross-coupling reactions, such as Heck arylation and Suzuki–Miyaura reactions (Suzuki coupling), has been much debated in recent years[1] following observations that such commercially important chemistry is not confined to homogeneous organometallic Pd complexes; condensed Pd phases, such as colloidal and supported nanoparticles,[2,3] are also able to mediate cross-coupling reactions. There is considerable circumstantial evidence that in the latter materials, surface sites may play a direct role in the catalytic cycle.[4]

The existence and relative importance of heterogeneous versus homogeneous pathways is significant for two reasons.[5,6] First, there remains a fundamental debate as to whether the active species in palladium-mediated cross-coupling reactions always involves low-nuclearity Pd, or in stark contrast, is entirely heterogeneous (operates over a solid surface) in nature.[3,6,7] Second, the need for alternative clean technologies operable as continuous-flow processes is driving the search for stable, solid catalysts able to activate and couple organohalides under mild conditions. Despite many ex situ microscopic and kinetic studies, unequivocal evidence for surface-catalyzed cross-coupling chemistry remains elusive. The lack of such evidence reflects the difficulty in remotely monitoring the structure of nanoparticulate materials during liquid-phase reactions without, for example, risking perturbation by invasive chemical/electrical probes. Narayanan and El-Sayed[8] and Bradley and co-workers[9] have suggested that low-coordination sites on polymer-stabilized Pd nanoparticles may play a key role in Suzuki coupling and Heck arylation, although it is postulated that these sites may simply act as a reservoir of active, soluble molecular palladium.[6,10] The latter hypothesis is largely founded on reports by several research groups of an unexpected inverse correlation between palladium loading and catalyst-turnover frequency, wherein dilution is believed to prevent agglomeration into unreactive Pd^0 clusters.[11,12] In a recent elegant study, a nanoporous alumina membrane was used to demonstrate that (at least for 15 nm Pd nanoparticles stabilized by tetraoctylammonium glycolate), catalytic Heck and Sonogashira coupling must be driven by palladium moieties of less than 5 nm in diameter released from larger parent clusters.[13] Although this finding may reflect leaching of soluble Pd atoms, the possibility that the observed catalysis resulted from the transport of small Pd nanoparticles (of a size examined in the present study) across the membrane cannot be entirely discounted. The most compelling evidence for surface-driven Suzuki coupling derives from an ingenious experiment in which Davis and co-workers used a palladium-nanoparticle-coated AFM probe to initiate spatially controlled coupling over surface-tethered aryl halides or styrene;[14] such a highly localized reaction would be unexpected if coupling were indeed mediated by mobile, solubilized Pd species diffusing freely throughout the solvent media.

In this study, we utilized XAS to quantitatively track the local structure of monodispersed Pd nanoparticles during a Suzuki coupling reaction. By following the local coordination environment in an operando mode (real-time measurement under working conditions),[15] we found strong evidence that their reactivity is indeed heterogeneous in origin and associated with the presence of stable surface defect atoms.

A series of polyvinylpyrrolidone-stabilized Pd nanoparticles, the mean diameter of which ranged from 1.8 to 4.0 nm, were prepared as described in the Experimental Section. Bulk and surface elemental analysis (see the Supporting Information) confirmed that these nanoparticles contained low metal concentrations and that the polymer composition remained unchanged. High particle uniformity was verified by electron microscopy, which in conjunction with powder X-ray diffraction and surface-sensitive X-ray photoelectron spectroscopy (see the Supporting Information) confirmed the successful synthesis of Pd^0 nanoparticles with truncated cubeoctahedral morphologies. The Suzuki coupling of iodoanisole (**1**) with phenylboronic acid (**2**) was monitored over a family of nanoparticles stabilized by polyvinylpyrrolidone (PVP) while Pd K-edge XAS spectra were acquired by fluorescence by using a purpose-built cell with a detector (Figure 1).

The resulting catalytic activity (derived from reaction profiles in the Supporting Information) is expressed as the turnover frequency (TOF) as a function of nanoparticle size in Figure 2. To identify any structure sensitivity (i.e. preference for a particular ensemble[16,17]), we normalized these TOF values to either the total number of surface Pd atoms or only those in five- or six-coordinate sites (so-called defects).[18] The sharp fall in TOF with nanoparticle size per

---

[*] Dr. K. Wilson, Prof. A. F. Lee
School of Chemistry, Cardiff University
Cardiff CF10 3AT (UK)
E-mail: leeaf@cardiff.ac.uk
Homepage: http://www.cardiff.ac.uk/chemy/contactsandpeople/academicstaff/lee.html
Dr. P. J. Ellis, Prof. I. J. S. Fairlamb, Dr. S. F. J. Hackett
Department of Chemistry, University of York
York YO10 3EY (UK)
E-mail: ijsf1@york.ac.uk

[**] We thank the EPSRC (EP/E046754/1, EP/G007594/1), the ESRF (award CH2432), AstraZeneca, and the Royal Society for supporting this research, and Dr. S. Nikitenko for assistance on beamline BM26. XAS = X-ray absorption spectroscopy.

Supporting information for this article is available on the WWW under http://dx.doi.org/10.1002/anie.200906675.

© 2010 Wiley-VCH Verlag GmbH & Co. KGaA, Weinheim

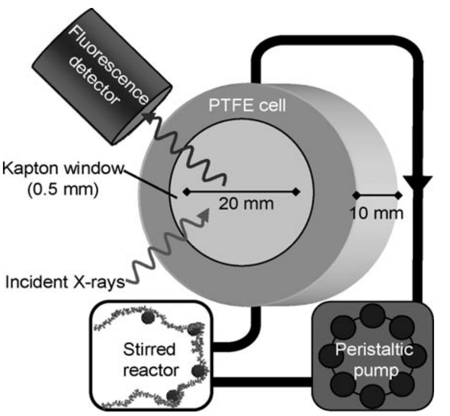

Figure 1. Recircultaing reactor setup for operando fluorescence XAS. A solution of PVP-stabilized Pd nanoparticles (50 ppm metal) is flowed through the cell during spectral acquisition while the reactor is simultaneously sampled for off-line GC analysis. PTFE = Teflon.

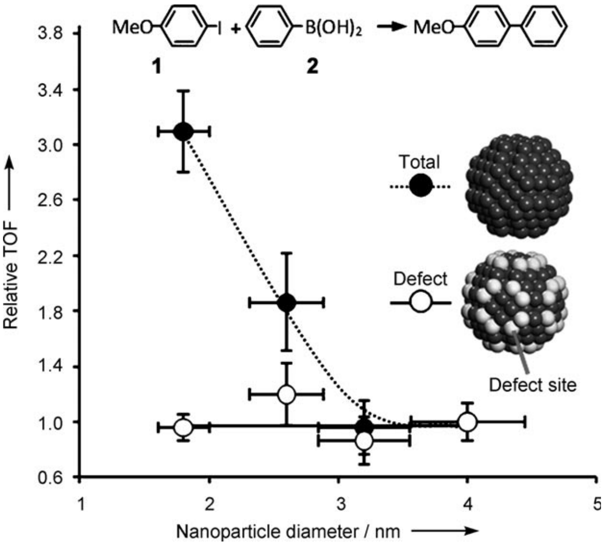

Figure 2. Structure-sensitive Suzuki coupling of **1** and **2** over size-selected, cubeoctahedral, PVP-stabilized Pd nanoparticles. Turnover frequencies are normalized relative to the surface-atom densities of the largest nanoparticle: total surface atoms (●) or defect surface atoms (○). The normalized cross-coupling rate should be independent of nanoparticle size if the correct active site has been identified.

surface Pd atom is characteristic of preferential reaction over specific active surface sites. Indeed, this size dependence is eliminated when the coupling rate is normalized to surface atoms that only occupy edge and vertex positions; that is, reactivity is associated with surface defect atoms. However, it has been postulated that such correlations may simply reflect a greater propensity for low-coordinate Pd to solubilize and thereby promote homogeneous reactivity.[6] Nanoparticle stability and the potential leaching of such defect atoms was therefore probed simultaneously by operando XAS.

Normalized absorbance and chi spectra of the as-prepared materials, along with fitted radial-distribution functions and associated parameters, can be found in the Supporting Information. The average Pd–Pd coordination number (CN_{Pd-Pd}) is sensitive to both particle size and morphology, particularly for clusters only a few nanometers thick.[19] In comparing the extended X-ray absorption fine structure (EXAFS) intensities of such small monodispersed clusters, wherein the bond-length disorder is to a first approximation constant, the oscillation intensity for an individual atom can be taken as directly proportional to its local coordination number.[20] The cluster-average radial-distribution function is then simply the weighted sum over all atoms in the cluster. For a simulated 1.8 nm Pd cubeoctahedral particle comprising 236 atoms, the calculated mean first-shell CN_{Pd-Pd} value was 9.46, in excellent agreement with the observed value of 9.58 for the as-prepared nanoparticle.

The time-dependent variation of CN_{Pd-Pd} for the 1.8 nm nanoparticles is shown in Figure 3, which is derived from a selection of EXAFS snapshots (inset) during the reaction. It is immediately apparent that these nanoparticles are extremely stable under these reaction conditions:[21] neither sintering nor dissolution (which would induce a respective increase or decrease in CN) is evident. This stability was confirmed by high-resolution TEM, which showed no size or shape changes between fresh and spent nanoparticles (see the Supporting Information).

To evaluate the sensitivity of our XAS measurements to defect dissolution, spectra were simulated for the analogous 1.8 nm particle with all 48 Pd defect atoms removed into solution as square-planar monomeric species coordinated to C or O ligands. The resulting radial-distribution function and mean CN_{Pd-Pd} value can be derived by weighting these simulated spectra. Figure 3 (inset and main) shows that such leaching would lead to a drop in CN_{Pd-Pd} to 7.23, which far exceeds the experimental standard deviation of 0.24 and equates to a sensitivity to the loss of as few as 10 defect atoms per particle. This result enables us to place an upper limit on the concentration of leached Pd of only 0.03 mol% (versus 0.67 mol% initially added as PVP-stabilized Pd). Since the correlation in Figure 2 was obtained on the basis that all surface defects contributed to the coupling rate, we can also discount fluxional behavior (e.g. cycles of Pd dissolution, solution-phase catalysis, readsorption) involving a large fraction of available defect atoms. The absence of any induction period also indicates that nanoparticulate palladium is not simply a precatalyst to the active species in the reaction, and is consistent with the constant measured particle size throughout the reaction. There is therefore no evidence for the solubilization, and homogeneous contribution, of significant molecular Pd species in our system.

However, to quantify the potential impact of trace dissolved Pd, we deliberately spiked a standard reaction with the maximum amount of $Pd(OAc)_2$ that could have passed undetected in our XAS experiments (0.03 mol%); if the catalysis observed under standard conditions predominantly reflects leached defect atoms, then spiking with additional soluble Pd should dramatically enhance activity. In fact, no benefit from this additional source of homogeneous palladium was observed (Figure 4); hence, such small amounts of leached Pd cannot account for the observed reactivity in this system. This finding is supported by

© 2010 Wiley-VCH Verlag GmbH & Co. KGaA, Weinheim

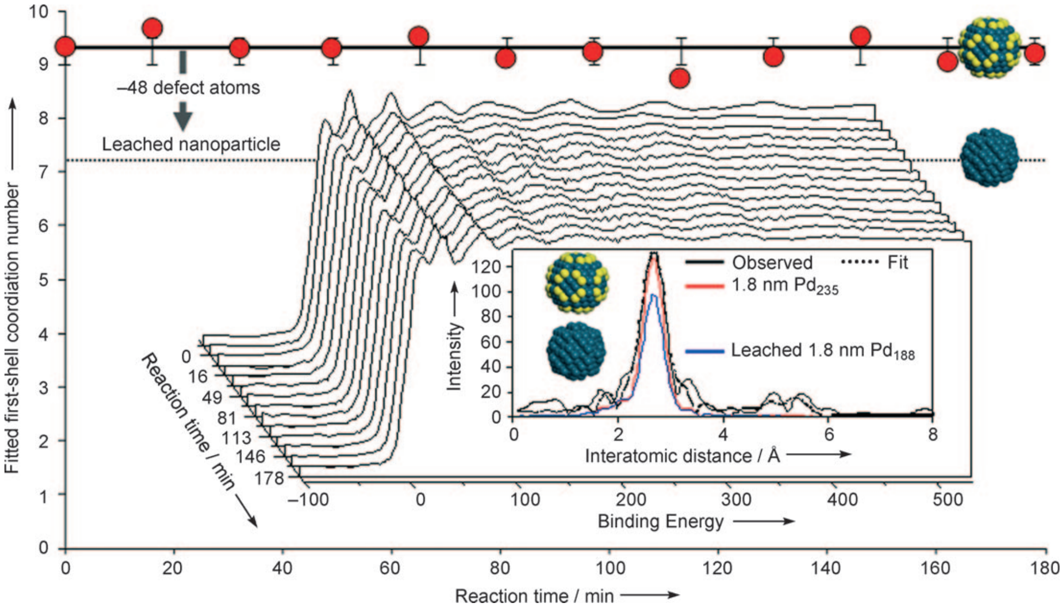

Figure 3. Operando Pd K-edge XAS fits of 1.8 nm PVP-stabilized Pd nanoparticles during the Suzuki coupling of **1** and **2**; error bars indicate standard deviation. The normalized, time-dependent EXAFS spectra and actual/simulated radial-distribution functions shown in the inset for as-prepared (236 atom) and leached (188 atom) Pd cubeoctahedra provide evidence for the preservation of the initial nanoparticle structure throughout the coupling reaction.

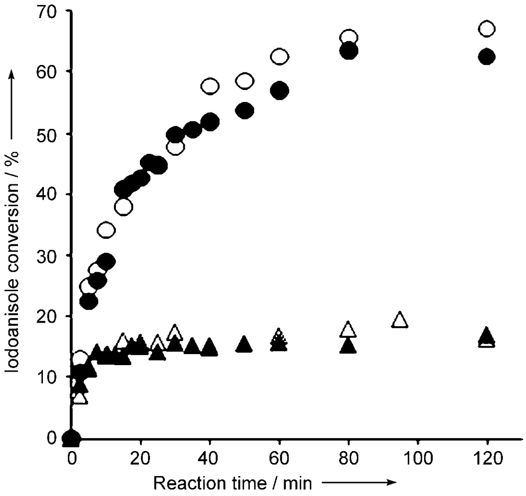

Figure 4. Reaction profiles for the Suzuki coupling of **1** and **2** over 1.8 nm PVP-stabilized Pd nanoparticles (0.67 mol% metal) ○; with $Pd(OAc)_2$ (0.03 mol%) added after 18 min ●; with Hg (10 equiv) added after 8 min △; or with Hg (10 equiv) added after 8 min, followed by $Pd(OAc)_2$ (0.03 mol%) after a further 10 min ▲.

subsequent poisoning experiments, in which the same 1.8 nm Pd nanoparticles were exposed to Hg after a reaction time of 8 min. Treatment with Hg in this way immediately inhibited further reaction (Figure 4). Since the utility of Hg as a selective poison for surface chemical processes is somewhat contentious,[22] the resulting nanoparticles were isolated and examined ex situ by X-ray photoelectron spectroscopy (XPS). A 1:1 correspondence was observed between the surface concentration of palladium and mercury atoms, which confirmed that poisoning was associated with full encapsulation of nanoparticle surfaces by a monolayer of Hg atoms (see the Supporting Information). Of course, if the observed reactivity arose from soluble molecular Pd species leached from (and in equilibrium with) the nanoparticles, then poisoning of the surface sites would also suppress any homogeneous activity. We therefore conducted a second spike test, in which $Pd(OAc)_2$ (0.03 mol%) was added 10 min after the reaction had been arrested by the addition of Hg. (As mentioned earlier, the maximum quantity of palladium that could dissolve from our nanoparticles and equilibrate in solution without detection is 0.03 mol%). If the reactivity of our nanoparticles was indeed due to Pd leached from defects, the activity should be rapidly regenerated upon spiking; no such recovery was observed.

We subsequently investigated the use of thiolated porous silicas to discriminate homogeneous from heterogeneous contributions. Thiol groups have been postulated as selective scavengers of soluble palladium species liberated from nanoparticles during reaction.[6] We therefore compared the effect of the addition of Quadrasil MP on activity with that of the addition of two unfunctionalized silicas part way through a reaction (Figure 5).

Quadrasil MP and flash silica have identical pore-size distributions and surface areas (see the Supporting Information), and both wide-pore silicas proved equally effective at hindering the reaction. This suppression is therefore clearly unrelated to the presence of surface thiols and associated selective trapping of soluble Pd. Indeed, TEM, XAS, and XPS of these postreaction silicas (see the Supporting Information) demonstrated conclusively that these silicas do not select for soluble palladium, but rather hinder reaction by entraining parent nanoparticles within their pore network, which could result in severe mass-transport limitations and much slower

© 2010 Wiley-VCH Verlag GmbH & Co. KGaA, Weinheim

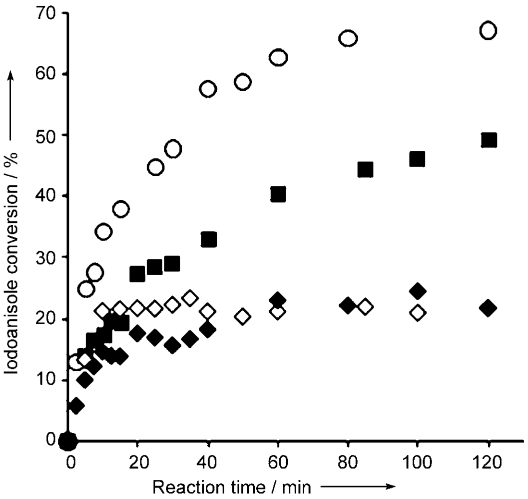

Figure 5. Reaction profiles for the Suzuki coupling of **1** and **2** over 1.8 nm PVP-stabilized Pd nanoparticles (0.67 mol% metal) ○; with Quadrasil MP (S/Pd 6:1, 40 mg) added after 10 min ◇; with flash silica (60 Å, 40 mg) added after 10 min ◆; or with MCM-41 (40 mg) added after 10 min ■.

reaction kinetics (but not true poisoning). This hypothesis is supported by the observation that despite its higher surface area, MCM-41 (with a pore diameter of only 2 nm) was less effective at retarding the reaction. Our observations negate the argument that Figure 5 simply reflects the nonspecific adsorption of active, dissolved Pd species at any silica surface; in that case, MCM-41 should be the greatest suppressant. If the Suzuki coupling were catalyzed homogeneously, Pd should be able to leach from such intraporous nanoparticles and move into the bulk medium to continue reaction. The presence of silicas in this series of reactions therefore provides further indirect evidence for surface-driven catalysis.

Additional (albeit indirect) evidence for a heterogeneous coupling was obtained from a comparison of the reaction kinetics of our 1.8 nm PVP-stabilized nanoparticles versus $Pd(OAc)_2$. Rate plots (see the Supporting Information) revealed that the coupling is first order in [Pd] for the nanoparticles, as required for a surface process; in contrast, a strong negative-order dependence was observed with the acetate (as reported by many research groups; such a process is sometimes termed homeopathic catalysis). This phenomenon highlights a striking difference between the solid and molecular systems and has been attributed to the tendency of low-nuclearity Pd species to aggregate and form “inert nanoparticulate reservoirs” as the palladium concentration increases. If the reactivity in our system indeed arose from dissolved Pd, then one would expect coupling rates to likewise decrease with an increasing PVP–Pd-nanoparticle loading; we observed the opposite in our study.

In conclusion, a combination of operando XAS, surface-sensitive XPS, and detailed kinetic profiling has provided the first direct evidence that Suzuki coupling can occur heterogeneously, at the surface of PVP-stabilized Pd^0 nanoparticles. Ongoing computational and experimental vacuum studies over model single-crystal surfaces will hopefully shed additional light on the coordination mode of the aryl halide and the organoboronic acid, and lead to the identification of the rate-limiting step. In time, this discovery may pave the way for the design of shape-selected and alloy nanoparticles with enhanced activity and durability for Suzuki, and possibly other palladium-mediated, cross-coupling reactions.

Experimental Section

PVP-stabilized Pd nanoparticles were prepared on the basis of previously described literature methods.[9,23] Briefly, an aqueous solution (240 mL) of H_2PdCl_4 (2.0 mmol) was refluxed under air with deionized H_2O (224 mL), ethanol (Fisher, HPLC grade, 336 mL), and PVP (Aldrich, molecular weight 29000, 1.067 g) for 3 h to produce a palladium seed. Larger particles were synthesized by the stepwise growth of this seed solution through the addition of an equivalent volume of a solution of H_2PdCl_4 (0.6 mmol) in a 2:3 ethanol/water mixture and further heating at reflux under air for 3 h. This process was repeated to produce nanoparticles of four different sizes. Water and ethanol were subsequently removed by ultracentrifugation and rotary evaporation, and the nanoparticles were dried at 70 °C under air for 12 h and then stored in air prior to use.

Elemental analysis was carried out by atomic absorption spectrometry with a Hitachi Z-5300 spectrophotometer. XRD spectra were recorded on a Bruker AXS D8 diffractometer with a $Cu_{K\alpha}$ X-ray source. TEM images were recorded on an FEI Tecnai 12 Biotwin high-contrast microscope and JEOL 2010 microscope, both at 120 keV. Surface analysis was performed on a Kratos HSi XPS system with a monochromatic $Al_{K\alpha}$ source (1486.6 eV) at normal emission and 40 eV pass energy; the energy was referenced to the valence band and adventitious carbon. CasaXPS2.3.15 was used for spectral fitting. Ex situ transmission Pd K-edge (24.35 keV) spectra were acquired at Station 9.3 of the Daresbury SRS on samples in stainless-steel washers. Operando XAS measurements were acquired every 5 min on beamline BM26 of the ESRF by using a purpose-built PTFE fluorescence flow cell linked to an external glass reactor. Reaction mixtures were circulated through the cell at 60 °C (see the Supporting Information). The Pd concentration was 50–200 ppm (depending on the nanoparticle size). X-ray absorption near edge structure (XANES) spectroscopic analysis was conducted with IFFEFIT Athena software. EXCURV98 was used for EXAFS fitting. 4-Iodoanisole (10.0 mmol) was placed in a 50 mL round-bottom flask and purged with N_2. A solution of mesitylene (1 mmol; internal standard) in toluene (Fisher, HPLC grade, 50 mL) was then added, and the resulting mixture was stirred. Phenylboronic acid (15 mmol), $KOCH_3$ (20 mmol), and the Pd nanoparticles (0.20 g) were placed in a separate flask under N_2, and CH_3OH (50 mL) was added. Both flasks were heated under thermostat control at 60 °C, and the Pd methanolic solution was then transferred into the main reaction vessel containing PhI to initiate the reaction. Reaction profiles were obtained by the periodic sampling of 0.1 mL aliquots, which were filtered through a 1 cm^3 silica bed and eluted with CH_2Cl_2 prior to analysis on a Varian CP3800 GC instrument with a DB5 column (30 m × 0.25 mm). The error in the GC conversions measured is ± 2%.

Received: November 26, 2009
Published online: February 2, 2010

Keywords: C–C coupling · EXAFS spectroscopy · heterogeneous catalysis · palladium · surface analysis

---

[1] a) *C&E News* **2004**, *82*(36), 49–58; b) Special Issue on “Cross Coupling”: Ed: S. L. Buchwald, *Acc. Chem. Res.* **2008**, *41*, 1439–1564.
[2] R. L. Augustine, S. T. O’Leary, *J. Mol. Catal.* **1992**, *72*, 229–242.

© 2010 Wiley-VCH Verlag GmbH & Co. KGaA, Weinheim

[3] L. Durán Pachón, G. Rothenberg, *Appl. Organomet. Chem.* **2008**, *22*, 288–299.

[4] a) M. T. Reetz, E. Westermann, *Angew. Chem.* **2000**, *112*, 170–173; *Angew. Chem. Int. Ed.* **2000**, *39*, 165–168; b) M. T. Reetz, J. G. de Vries, *Chem. Commun.* **2004**, 1559–1563; c) J. G. de Vries, *Dalton Trans.* **2006**, 421–429.

[5] J. A. Widegren, *J. Mol. Catal. A* **2003**, *198*, 317-.

[6] T. S. N. Phan, M. Van der Sluys, C. W. Jones, *Adv. Synth. Catal.* **2006**, *348*, 609–678.

[7] R. Narayanan, C. Tabor, M. El-Sayed, *Top. Catal.* **2008**, *48*, 60–74.

[8] R. Narayanan, M. El-Sayed, *J. Phys. Chem. B* **2004**, *108*, 8572–8580.

[9] J. Le Bars, U. Specht, J. S. Bradley, D. Blackmond, *Langmuir* **1999**, *15*, 7621–7625.

[10] C. C. Cassol, A. P. Umpierre, G. Machado, S. I. Wolke, J. Dupont, *J. Am. Chem. Soc.* **2005**, *127*, 3298–3299.

[11] A. H. M. de Vries, J. M. C. A. Mulders, J. H. M. Mommers, H. J. W. Henderickx, J. G. de Vries, *Org. Lett.* **2003**, *5*, 3285–3288.

[12] I. J. S. Fairlamb, A. R. Kapdi, A. F. Lee, G. Sánchez, G. López, J. L. Serrano, L. García, J. Pérez, E. Pérez, *Dalton Trans.* **2004**, 3970–3981.

[13] M. B. Thathagar, J. E. ten Elshof, G. Rothenberg, *Angew. Chem.* **2006**, *118*, 2952–2956; *Angew. Chem. Int. Ed.* **2006**, *45*, 2886–2890.

[14] a) J. J. Davis, K. S. Coleman, K. L. Busuttil, C. B. Bagshaw, *J. Am. Chem. Soc.* **2005**, *127*, 13082–13083; b) J. J. Davis, C. B. Bagshaw, K. L. Busuttil, Y. Hanyu, K. S. Coleman, *J. Am. Chem. Soc.* **2006**, *128*, 14135–14141.

[15] a) B. M. Weckhuysen, *Phys. Chem. Chem. Phys.* **2003**, *5*, 4351–4360; b) M. A. Bañares, *Catal. Today* **2005**, *100*, 71–77; c) J. M. Thomas, J.-C. Hernandez-Garrido, *Angew. Chem.* **2009**, *121*, 3962–3965; *Angew. Chem. Int. Ed.* **2009**, *48*, 3904–3907.

[16] M. Boudart, *Adv. Catal.* **1969**, *20*, 153–166.

[17] R. A. Van Santen, *Acc. Chem. Res.* **2009**, *42*, 57–66.

[18] Total and defect site distributions were calculated by using Materials Studio 5.0, and XAS spectra were simulated by using the IFEFFIT 1.2.11 freeware suite.

[19] A. Jentys, *Phys. Chem. Chem. Phys.* **1999**, *1*, 4059–4063.

[20] a) A. I. Frenkel, C. W. Hills, R. G. Nuzzo, *J. Phys. Chem. B* **2001**, *105*, 12689–12703; b) A. I. Frenkel, *Z. Kristallogr.* **2007**, *222*, 605–611.

[21] Solvents, such as *N*,*N*-dimethylformamide, are more likely to promote solubilization; see, for example: T. E. Storr, A. G. Firth, K. Wilson, K. Darley, G. Baumann, I. J. S. Fairlamb, *Tetrahedron* **2008**, *64*, 6125–6137.

[22] J. A. Widegren, M. A. Bennett, R. G. Finke, *J. Am. Chem. Soc.* **2003**, *125*, 10301–10310.

[23] T. Teranishi, M. Miyake, *Chem. Mater.* **1998**, *10*, 594–600.

© 2010 Wiley-VCH Verlag GmbH & Co. KGaA, Weinheim